Inverse Photoionization Studied via Radiative Electron Capture into Highly Charged Ions

Th. Stöhlker[1,2], O. Brinzanescu[2,3], A. Krämer[1,2], T. Ludziejewski[2,4], X. Ma[2,5], P. Swiat[6], and A. Warczak[6]

[1] *Institut für Kernphysik, University of Frankfurt, 60486 Frankfurt, Germany*
[2] *Gesellschaft für Schwerionenforschung, 64291 Darmstadt, Germany*
[3] *National Institute for Laser, Plasma and Radiation Physics, 76900 Bucharest-Magurele, Romania*
[4] *Institute for Nuclear Studies, 05-400 Świerk, Poland*
[5] *Institute of Modern Physics, 730000 Landzhou, China*
[6] *Institute of Physics, Jagiellonian University, 30-059 Cracow Poland*

Abstract. Differential aspects of the photoelectric effect for high-Z hydrogen-like and few-electron ions are studied by the time-reversed process in ion-atom collisions, i.e. by radiative capture of a quasi-free target electron. In this time-reversed situation the capture of an electron into a bound state of the ion is accompanied by the simultaneous emission of a photon, allowing for a direct and unambiguous experimental access to this process. Therefore, radiative capture provides a unique tool to investigate the details of the photoionization process even in the case of high-Z highly charged ions where such investigations are currently not accessible in the direct channel. At high-Z relativistic effects become important for which photon angular distributions turn out to be a very sensitive probe. This was demonstrated very recently, by an angular distribution study performed for electron capture into the 1s ground state of U^{92+}. This particular experiment allowed us to identify spin-flip contributions to the photoionization process at large backward angles. Here, we review the shell and subshell differential photon-angular distribution studies for radiative capture into highly-charged uranium ions. The experimental data are compared with exact relativistic calculations giving detailed insight into the fundamental electron-photon interaction process involved.

INTRODUCTION

In relativistic atomic collisions between highly-charged heavy ions and low-Z target atoms *Radiative Electron Capture* (REC) is one of the most important reaction channels. Here, the coupling between the electron and the electromagnetic field of the fast moving projectile results in an electron capture into a bound state of the ion via simultaneous emission of a photon carrying away the energy and momentum difference between the initial and final electron states [1–4]. Consequently REC can be viewed as the time-reversed photoionization process as long as the initial electron momentum distribution in the target atom can be neglected, an excellent approach when dealing with relativistic encounters between high-Z projectiles and low-Z atoms [3].

Previously we have shown that for high-Z ions detailed information about the elementary photoionization process itself can be obtained via a study of its inverse reaction occurring in energetic ion-atom collisions [3,4,6]. In this domain of high-Z ions the photon-atom interaction is strongly influenced by relativistic effects [7]. For the exploration of such details, angular distributions are a very sensitive probe. For the nonrelativistic domain of low-Z ions, this has already been stressed by Krässig and coworkers, who observed nondipolar corrections to the photoeffect [8]. In contrast, at high-Z the full retarded multipole expansion of the photon field must be considered and the strength of relativistic effects may lead to considerable corrections. Evidently, the latter effects are of particular interest when dealing with high-Z ions [9]. However, they are difficult to observe in direct photoionization experiments, since retardation leads to a strong forward peaking of the photoelectron angular distribution. Moreover, REC provides most favorable conditions because it gives experimental access to the study of photoionization even for H-like high-Z ions, i.e. for an explicitly point Coulombic system. Most remarkably, as has been first pointed out by Spindler et al. [10], a cancellation between retardation and Lorentz transformation occurs for the angular distribution of REC into the K shell of bare ions. As a consequence, the $\sin^2\theta$ distribution of the simple nonrelativistic dipole-approximation is restored. Indeed a complete cancellation occurs as long as retardation is considered in all orders in a nonrelativistic treatment [10,11]. Therefore, deviations from the symmetric $\sin^2\theta$ distribution provide a direct measure of relativistic corrections. These deviations turn out to be rather unimportant at ion energies up to 300 MeV/u and nuclear charges up to $Z = 50$ or 70 [12]. However, at these energies and for $Z = 92$ a significant cross section at forward angles has been predicted for REC into the K shell [3,12,13] and has been shown to be a unique signature of spin-flip transitions. Besides this unique aspect of the time-reversed situation, further peculiarities must be mentioned. By means of REC, photoionization can be studied even for excited states in high-Z H-like ions. Most important, no corrections due to electron scattering occurring in solid targets are required, leading in conventional photoionization studies for high-Z elements to a considerable broadening of the electron emission angle [14]. The absence of the these corrections in REC experiments allows one to extend photoionization studies to much lower energies than available for the direct channel. For a review of the photoionization experiments at high-Z we refer to [7,15].

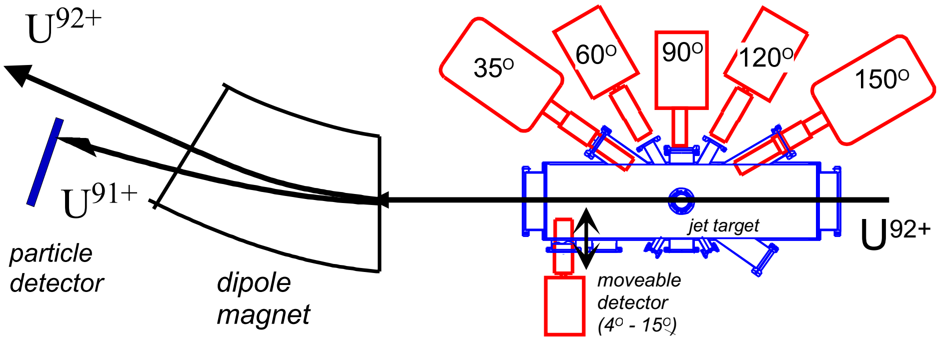

FIGURE 1. Layout of the experimental arrangement at the ESR-jet target. Various x-ray detectors view the target interaction zone at observation angles ranging from almost 0° to 150°. Photon emission is observed in coincidence with the down-charged ions, detected in a particle counter located behind the dipole magnet.

EXPERIMENTAL TECHNIQUE

In the following we concentrate on the most recent experiments conducted at the relativistic heavy-ion storage ring ESR at GSI in Darmstadt [16]. This electron-cooler ring provides the basis for atomic-collision experiments dealing with beams of unprecedented quality [4,17–19]. At the ESR, the interaction of intense beams of cooled high-Z ions with low-dense gaseous matter can be studied without any beam collimation, guaranteeing almost completely background-free experimental conditions. Typically, the beam diameter is close to 1 mm and the gasjet target density amounts to about 10^{12} particle/cm^3 [20], compared to 10^{21} particle/cm^3 of solid-state targets. Nevertheless, due to the high revolution frequency of the ions of about 10^6 s^{-1}, even collision processes with tiny reaction cross-sections (0.1 barn or even smaller) became accessible by experiments. Until now, most atomic-collision studies at the ESR were concentrating on the study of x-ray emission occurring in relativistic collisions [4,17,21]. In Fig. 1, a scheme of the present experimental arrangement at the ESR gas-jet target is depicted. With this setup complete angular distribution studies are now accessible for the first time. Various x-ray detectors viewing the gas-jet/beam interaction zone at different observation angles whereby covering the range from almost 0° to almost 180° [22]. In addition, the dipole magnet accomplish to analyze the charge states of the emerging projectiles and the x-ray emission can be measured in coincidence with the down-charged projectiles (U^{91+}). A typical x-ray spectrum associated with electron capture is displayed in Fig. 2 which was obtained at an observation angle of 150° for 310 MeV/u $U^{92+}\rightarrow N_2$ collisions. Beside the Lyman ground-state transitions (Lyα_1: $2p_{3/2}\rightarrow 1s_{1/2}$, Ly$\alpha_2$: $2p_{1/2}\rightarrow 1s_{1/2}$, **M1**$2s_{1/2}\rightarrow 1s_{1/2}$) the most prominent features observed in the spectrum are due to radiative electron capture into the ground and excited projectile states. The width of these lines reflect the Compton profile of the bound target electrons (see e.g. [17]).

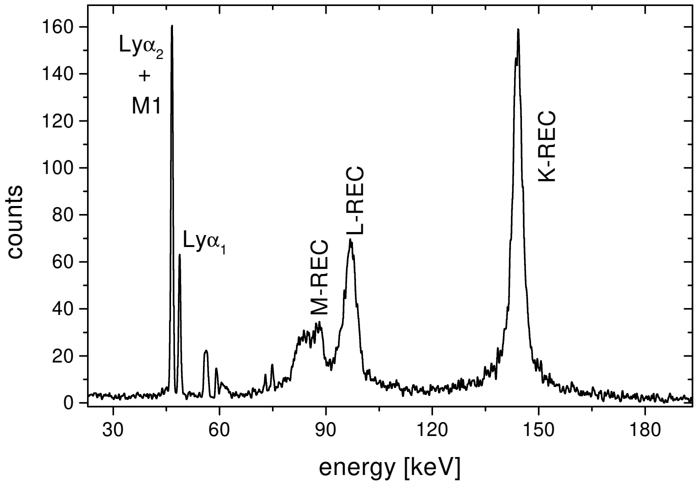

FIGURE 2. X-ray spectrum observed at nearly 150° for $U^{92+} \rightarrow N_2$ collisions at 310 MeV/u [22]. The data were taken in coincidence with down-charged U^{91+} ions [22].

In this most recent experiment we were aiming on a complete angular distribution measurement for REC into the ground-state of bare uranium (Z=92), i.e. the heaviest stable element. Until now, similar investigations for REC were restricted to Z$\leq$ 54. In the experiment, x-ray spectra were measured by using various Ge(i) and NaI x-ray detectors at in total six different observation angles covering the range from almost 0° to 150° [22]. Moreover, x-ray detection at almost 0° was accomplished by using a Ge(i) detector with four independent segments, each furnished with an individual readout. The horizontal and vertical size of each segment is 13 and 25 mm, respectively. The detector was mounted on a movable support, 510 mm down-stream from the projectile-target interaction region. Periodically, after the accumulation procedure was finished, the detector was positioned at a perpendicular distance of just 1 cm apart from the circulating beam. For the first stripe, this position corresponds to a mean observation angle of 4.6° with an angular acceptance of $\Delta\theta = \pm 0.7°$. Moreover, since the used Ge(i) detector possesses a good energy resolution (1.2 keV at 220 keV) but low detection efficiency for high photon energies (at almost 0° the K-REC centroid energy is close to 660 keV), we have also replaced the Ge(i)detector by an NaI counter which provides an improved detection efficiency by more than an order of magnitude. In Fig. 3, a coincident x-ray spectrum, measured with the innermost segment of the Ge(i)-detector is displayed along with the spectrum taken with the NaI counter. The mean observation angle of the latter detector corresponds to 6°. In both detectors, the K-REC line can be well identified at an x-ray energy of 660 keV. In addition, the Lyman transitions measured with the Ge(i) detector are shown separately in the inset, demonstrating the good energy resolution obtained. We have to stress that the almost background-free spectra observed close to 0° emphasize the brilliant beam conditions of the storage ring, which are in contrast to standard single-pass experi-

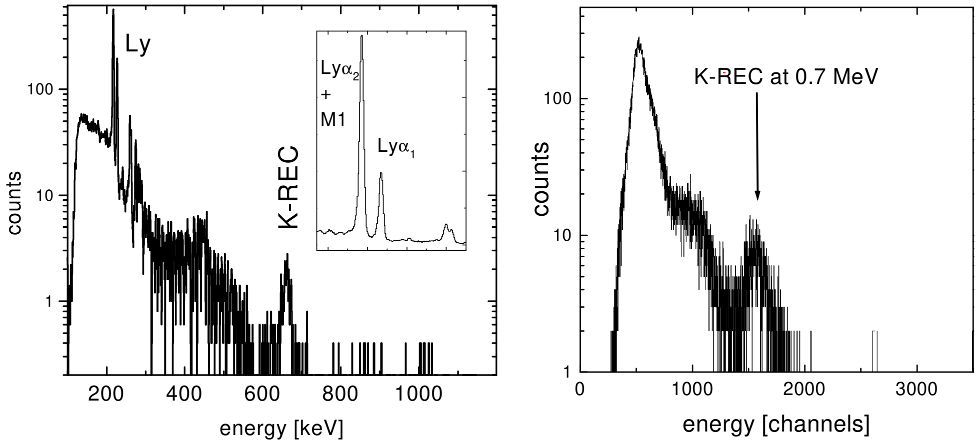

FIGURE 3. X-ray spectrum measured at nearly 0° for $U^{92+} \to N_2$ collisions at 310 MeV/u [22]. Spectrum at the right side: recorded with an NaI-detector; spectrum at the left side: recorded with a Ge(i)-detector.

ments with relativistic ion beams utilizing solid targets. There, the huge secondary electron production and its related bremsstrahlung prevents photon detection in the forward hemisphere.

K-Shell Angular Distribution for Hydrogen-Like Uranium: The Identification of Spin-Flip Transitions

In Fig. 4, the obtained differential cross section values are given as a function of the observation angle (for details of the data analysis we refer to Ref. [17,22]). In the figure the solid circles refer to the data obtained by the Ge(i) detectors whereas the open square depicts the result from the NaI counter. In addition, the data are compared with predictions based on rigorous relativistic calculations [12,13]. These calculations use exact relativistic bound-state and continuum wave functions and take into account all multipole orders up to about $L = 20$. In order to achieve convergence, the summation was carried out over all electron partial waves with Dirac quantum numbers $|\kappa| \leq 20$. For comparison, the measured angular distribution was normalized to the theoretical prediction at 90°. As seen in the figure, a good agreement between the experimental data and the rigorous relativistic theory is obtained. In order to reveal the necessity of such a complete relativistic treatment for high-Z projectiles we also depict in the figure the $\sin^2\theta$ distribution of the nonrelativistic theory which considers the full retardation as well as Lorentz transformation to the laboratory frame. Obviously, the experimental data deviate considerably from symmetry around 90°. Most important, the large cross section observed close to 0° disproves the nonrelativistic theory which predicts that 0° photon emission for REC into states with angular momenta ℓ =0 is forbidden due to angular momentum conservation. In a complete relativistic treatment, however,

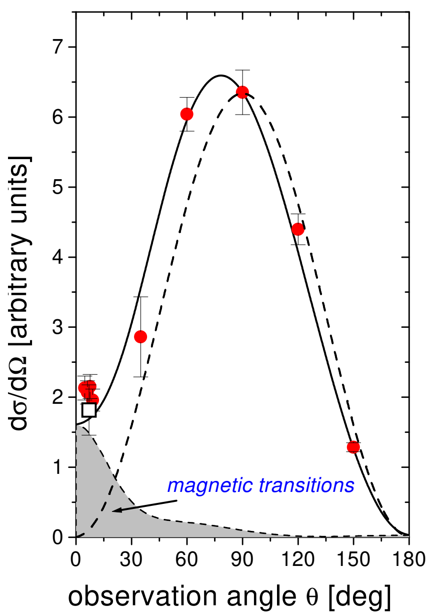

FIGURE 4. Angular distribution for REC into the K shell of bare uranium (solid circles) as a function of the observation angle θ (310 MeV/u $U^{92+} \rightarrow N_2$). The solid line depicts the complete relativistic calculations and the shaded area refers to the spin-flip contributions [13,12]. The $\sin^2\theta$ shape of the nonrelativistic dipole-approximation is given by the dashed line.

the interaction of the electron magnetic moment with the magnetic field produced by the fast moving projectile can produce spin-flip transitions which compensate the angular momentum carried by the photon.

Consequently, our measurement close to 0° provides a clear identification of spin-flip transitions occurring in relativistic ion-atom collisions. This effect has been predicted by Eichler et al. [11,12] pointing out that its differential cross section is a precise probe for theoretical wave functions. However, until now, this effect was confirmed experimentally. Even for the case of $Xe^{54+} \rightarrow$Be collisions at 197 MeV/u [23], no relativistic effects were observed and the measured K-REC angular distribution could be well reproduced by the nonrelativistic theory. We also have to emphasize that for high-Z ions our finding points to the importance of treating REC in all orders of αZ. Considering the relativistic Sauter approximation, where the interaction between a free electron and a bare ion is treated in lowest order of αZ, also the spin-flip contributions disappear at 0°.

In order to reveal the physics of the REC process and its relation to photoionization in more detail, we normalized the measured K-REC x-ray yield to the intensity of the simultaneously observed Ly-α_2+**M1** line. Since the Ly-α_2 and the **M1** transitions stem from the decay of the $2p_{1/2}$ and the $2s_{1/2}$ level, the corresponding line intensity follows an isotropic emission characteristic in the emitter frame. By applying this technique of normalization, the REC angular distribution in the emitter frame can be derived directly from the x-ray spectra. For this purpose only the Lorentz transformation of the observation angle is required (see e.g. Ref. [11]). The

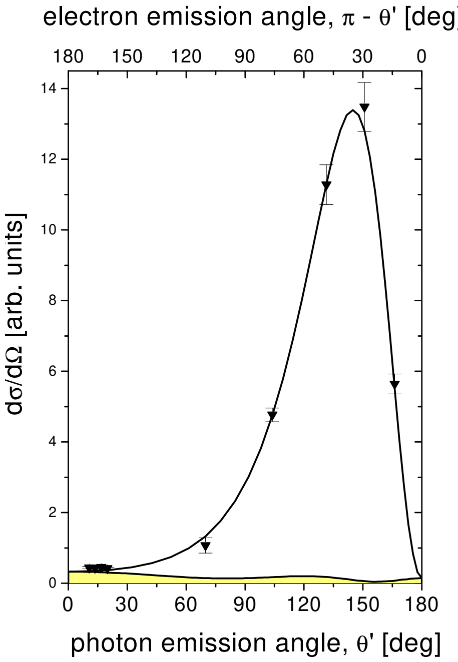

FIGURE 5. K-REC angular distribution (projectile frame) as a function of the emission angle θ' (bottom x-axis). The x-axis at the top refers to the corresponding electron angular distribution for photoionization of H-like uranium (photon energy 302 keV) obtained by the interchanging θ' by $\pi - \theta'$. The full line gives the photoionization distribution as obtained from complete relativistic calculation whereas the shaded area depicts the spin-flip contribution [22].

additional advantage of this technique is that also the uncertainty caused by the solid angle determination cancels out completely. In Fig. 5, the result for this ratio is depicted as a function of emission angle in the emitter frame (compare lower x-axis) along with the corresponding prediction by the rigorous relativistic theory. As can be observed in the figure, both the experimental and the theoretical angular distributions, exhibit a pronounced backward shift, since the strong retardation effect is no longer cancelled by the Lorentz transformation. The maximum of the distribution is now localized close to 150° and the cross section decreases drastically by more than an order of magnitude towards 0°. Here, indeed the occurrence of spin-flip transitions (compare shaded area in Fig. 5) appears to be a tiny effect with an almost isotropic emission characteristic. This is in obvious contrast to the discussed distribution in the laboratory frame where the Lorentz transformation not only compensates retardation but also amplifies the relative weight of the spin-flip transitions close to 0° with respect to the maximum of the distribution.

From the experimental REC distribution in the emitter frame the corresponding angular distribution for photoionization can also be derived. For this purpose the REC angle θ' has simply to be replaced by $\pi - \theta'$. This transformation is needed, because in relativistic ion-atom collisions, the quantization axis is determined by the direction of the projectile momentum. This is opposite to the direction of the electron (or photon) momentum as seen from the projectile. As a consequence, Fig. 5 refers also to the electron angular distribution for photoionization of H-like uranium at the corresponding photon energy of 302 keV whereby the angular transformation is given by the upper x-axis. This presentation illustrates the potential of REC experiments for precision studies of the photoionization process. In particular, it reveals the origin of the observed spin-flip transition as events related to large angle backward scattering in photoionization, i.e. where the momentum transfer to the nucleus is largest. Note, that this effect was not observed in direct photoionization experiments for high-Z ions. On the contrary, spin-flip contributions in the direct channel were observed at almost 0° (corresponding to 180° in the time reversed situation) at much larger energies.

Radiative Capture into Excited States

Radiative Capture into L-subshells

By means of REC, photoionization can also be studied for excited states in highly-charged heavy ions [6]. Here high-Z ions are of particular interest since the large fine structure splitting provides direct experimental access even for the investigation of angular distributions associated with REC into the j sublevels of the L shell.

For the first experimental study of the angular distributions for REC into the L-shell sublevels, He-like uranium was chosen as a projectile which can be produced with sufficient intensities even at an energy of as low as 89 MeV/u(corresponding to photoionization at 79 keV). Since the width of the target Compton profile decreases with decreasing beam energy [17], the low beam energy allowed us to resolve the fine structure components of the L shell of uranium. Note, that at such low photon energies, photoionization experiments for high-Z elements are presently not possible.

The results obtained within this experiment, conducted at the GSI Fragment Separator for $U^{90+}\rightarrow C$ collisions, are depicted in Fig. 6. In the figure the measured angular distributions for REC into the j=1/2 and j=3/2 levels of the L shell of He-like uranium are plotted in comparison with the predictions of the exact relativistic theory. The data for capture into the j=1/2 levels show a considerable bending of the angular distribution into forward direction whereas the distribution for capture into the pure p-state (j=3/2) exhibit a slight enhancement at backward angles. An excellent agreement between measurement and relativistic theory is found for both fine-structure components [24]. This result demonstrates that for p-states the Lorentz transformation is not sufficient to cancel the backward shift caused by retardation as in the case of s-states. On the contrary, the observed slight forward shift for capture into the $j = 1/2$ levels is caused by REC into the $2s_{1/2}$ state which is partially caused by spin-flip transitions. As shown in Ref. [24], the application of a non-relativistic treatment for the time reversed photo-effect yields strong deviations

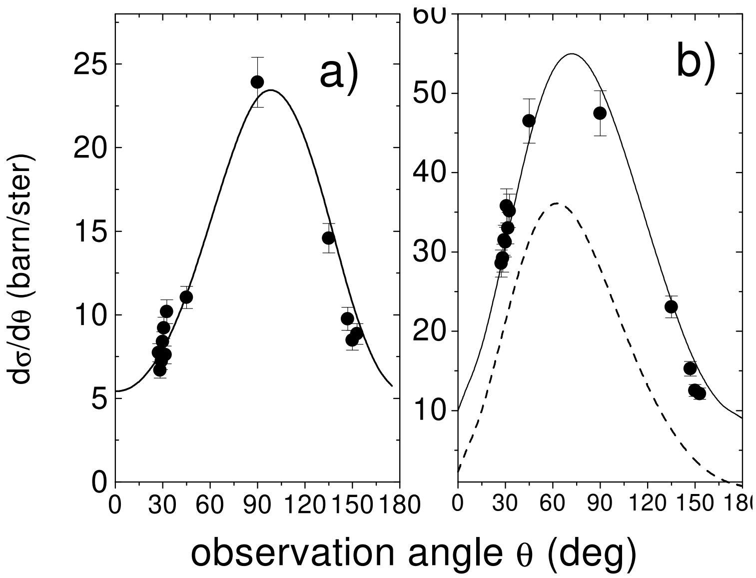

FIGURE 6. Experimental angular distribution of L-REC radiation for (a) REC into the $2p_{3/2}$ level and (b) for the $2s_{1/2}$ and $2p_{1/2}$ states. The solid line shows the result derived from exact relativistic calculations. The theoretical result for capture into the $2s_{1/2}$ state (dashed line in (b)) is shown separately.

especially in forward and backward directions. Again, these findings point out that angular differential REC cross-sections are extremely sensitive to details of the atomic wave functions.

Time-Reversed Two-Step Photoionization - Alignment of the $2p_{3/2}$ State Caused by Radiative Capture

In the following, we consider the inverse of a two-photon/one-electron ionization process. Here, the first photon resonantly excites an electron from the $1s_{1/2}$ ground state into the $2p_{3/2}$ hydrogen-like state and, subsequently, the second photon ionizes the excited electron within the lifetime of the $2p_{3/2}$ state, i.e. for the case of H-like uranium a time of the order of 10^{-17} s. We are interested in the magnetic subshell population of REC into the $2p_{3/2}$ state. Usually, information about degenerated atomic states, which differ only in their magnetic quantum number, is obtained by polarization measurements. However, since for high-Z ions like uranium the Lyα_1 transition energy appears close to 100 keV, a polarization measurement is almost impossible. The alignment of the $2p_{3/2}$ state and consequently its magnetic-substate population can also be deduced from an angular distribution measurement. Since the $2p_{3/2}$ decays by an **E1** transition to the ground state, the anisotropic emission in the emitter frame is simply given by [25]

$$I(\theta) \propto 1 + \beta_A \cdot [1 - \frac{3}{2}\sin^2\theta] \qquad (1)$$

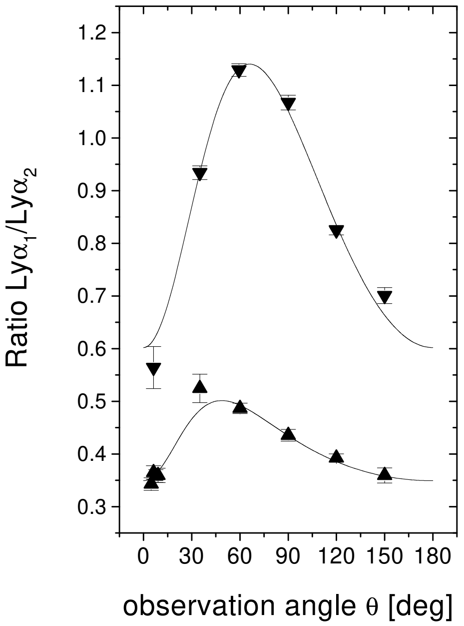

FIGURE 7. Experimental Lyα_1/Lyα_2 intensity ratio (solid triangles) measured for $U^{92+} \rightarrow N_2$ collisions (up-triangles: 310 MeV/u; down-triangles: 79 MeV/u). The lines depict the results of a least square adjustment of Eq. (1) to the experimental data [6].

where θ denotes the emission angle in the projectile frame and β_A gives the coefficient of the alignment which is related to the population cross-sections $\sigma(j, m_j)$ for the magnetic sublevels [25]

$$\beta_A = \frac{1}{2} \cdot \frac{\sigma_{(3/2,3/2)} - \sigma_{(3/2,1/2)}}{\sigma_{(3/2,3/2)} + \sigma_{(3/2,1/2)}}. \tag{2}$$

Consequently, by measuring the Lyα_1 emission at only a few observation angles, the relative population of the magnetic sublevels can be experimentally determined.

Such investigations were performed recently with bare Pb^{82+} and U^{92+} projectiles at the gas-jet target of the ESR storage ring [6]. In order to reduce possible systematic uncertainties, we again took advantage of the close spaced, simultaneously observed Lyα_2+**M1** transitions, which are isotropic in the emitter frame. By normalization to the latter, almost all systematic uncertainties cancel out. Moreover, the cascade population of the $2p_{3/2}$ state was investigated experimentally (see e.g. [6]) which was found to produce only Lyα_1 transitions. From the measured alignment of the $2p_{3/2}$-levels follows that about 75% of the capture events populate the $|m_j|=1/2$ sublevels of the $2p_{3/2}$ state which corresponds to a 40% linear polarization of the emitted Lyα_1 radiation. By subtracting the cascade contribution, we were able to deduce that direct radiative capture into the $2p_{3/2}$ state populates the $|m_j|=1/2$ magnetic sublevels by more than 90%. As a consequence, a surprisingly strong linear polarization by as much as 50% can be deduced from this finding. This result was derived from measurements at only three observation

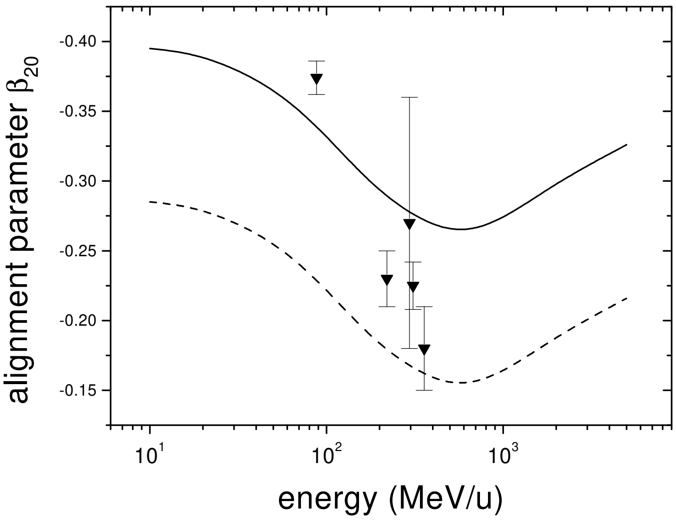

FIGURE 8. All alignment parameters β_{20} (down triangles) measured for the Lyα_1 radiation of U^{91+} produced in $U^{92+} \rightarrow N_2$ collisions as a function of collision energy. The full line refers to relativistic calculations of the alignment of the $2p_{3/2}$ assuming the time-reversal of two-step photoionization. The dashed line refers to the same calculations but considers in addition feeding transitions from higher excited levels. The latter were obtained from experimental data.

angles, exploiting the fact that the shape of the angular distribution is precisely known (see Eq. 1). During the most recent beam time with the new experimental setup (see above), however, we obtained also data for the alignment of the $2p_{3/2}$ in H-like uranium by a measurement in the angular range between nearly 0° and 150° ($U^{92+} \rightarrow N_2$ collisions at 310 MeV/u). In Fig. 7, the measured intensity distribution of the Lyα_1 radiation is depicted as function of the observation angle. In addition, the solid line depicts a least square adjustment of Eq. 2 to the experimental data points (upper triangles in Fig. 7). As a result, we obtain for the collision energy of 310 MeV/u a β_A parameter of -0.225 ± 0.017, in accordance with the former experimental findings for energies above 220 MeV/u [6]. However, for these high energies where REC is known to be the only relevant Lyα production process, all experimental alignment data appear to be in variance with complete theoretical *ab initio* calculations [25,26]. This is depicted in Fig. 8 where the theoretical and the experimental data are compared as a function of beam energy. In the figure, the solid line refers to the theoretical prediction of the alignment parameter for radiative capture into the $2p_{3/2}$ of H-like uranium [26]. The dashed line includes in addition feeding transitions from higher excited levels and should be compared with the experimental observation for energies above 200 MeV/u. Although this correction was derived from the experimental data, the cascade contributions might be responsible for the found deviations.

Already at high energies (above 200 MeV/u) the observed alignment of the $2p_{3/2}$ is surprisingly strong. On the other hand, we observed an even more pronounced and almost complete alignment (β_A=-0.374 ± 0.012) of the $2p_{3/2}$ state in U^{91+} for decelerated U^{92+} ions in collisions with N_2 molecules (compare also Fig. 7). At this low-energy the competing non-radiative electron capture process can no longer be neglected. Since we expect for this process an almost statistical population of the magnetic sublevels, the reason for the almost complete alignment observed for decelerated ions appears to be unknown.

OUTLOOK AND SUMMARY

In summary, the fundamental interaction process between an electron and a photon in the presence of a strong central atomic field is discussed from the point of view of radiative electron capture into highly-charged uranium ions. In particular the REC cases studied for bare U^{92+} ions show the unique potential of these investigations in order to elucidate the subtleties of the photoionization process for bare high-Z ions where the interaction can be studied for explicitly point Coulombic systems. The angular distribution studies discussed benefit in particular from the partial cancellation of retardation which arises from relativistic transformations from the emitting fast ion system into the laboratory frame. As a consequence, deviations from the $\sin^2\theta$ distribution turn out to be a very sensitive probe for relativistic corrections to the angular distribution for photoionization. The sensitivity of this technique is illustrated by the experimental separation and identification of spin-flip contributions to the angular-differential cross-section at the correspondingly photon energy of 302 keV for the time-reversed process. At such low-energies this effect was not accessible up to now in direct photoionization studies. Moreover, the structure of the photon spectra allows us to clearly differentiate between radiative capture into the ground state and into higher shells. For the L-shell even the fine-structure components are resolved in the REC spectra, providing an additional differentiation among the j values of the L-levels ($2s_{1/2}$ and $2p_{1/2}$ as well as $2p_{3/2}$). Here, the experimental results underline the importance of the angular momentum of the final state. In particular, the data confirm relativistic calculations that for capture into p-states retardation effects show up more pronounced compared to s-states, i.e. in contrast to s-states retardation is not canceled by the Lorentz transformation. Furthermore, even the magnetic substate population of the time-reversed double-photoionization could be addressed by the experiments. Here, a surprisingly strong linear polarization (almost 40%) of the emitted Lyα_1 photons was deduced from the anisotropy of the measured angular distribution. However, in this particular case, the experimental data deviations is found to be in variance with theory. Additional studies are required in order to solve this issue.

In the near future we like to extend these studies to decelerated high-Z ions. This will allow us to perform experiments where in the time-reversed situation the corresponding photon energy is close to threshold, i.e. an energy regime where no data for photoionization of high-Z elements exists. Moreover, we like to concentrate on high-Z few electron systems where the spin coupling in multi electron systems must be considered in addition. Up to now our experimental findings confirm theoretical

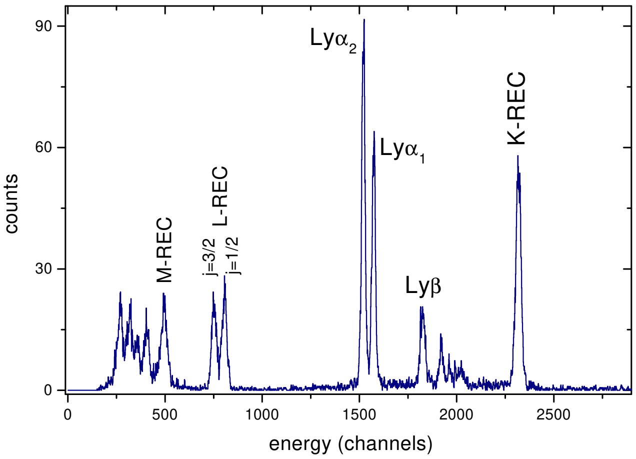

FIGURE 9. X-ray spectrum of Pb^{81+}, produced in collisions of strongly decelerated Pb^{82+} projectiles with H_2 molecules at 25 MeV/u [27]. The spectrum was measured at an observation angle of 150°.

predictions that for K-shell photoionization neither screening effects nor electron correlations are of importance at high energies. However, for high-Z few electron ions at low energies the situation is not clear. As a prerequisite the deceleration mode at the ESR could already be established which allowed us very recently to decelerate bare gold ions (Z=79) to energies of as low as 25 MeV/u (corresponding to an electron moving with a kinetic energy of 13 keV in the projectile frame). In addition, a H_2 cluster jet-target was commissioned at the ESR [27]. As a result, x-ray spectra with an extremely narrow REC line-profile could be measured (compare Fig. 9).

This work was done in collaboration with F. Bosch, R.W. Dunford, C. Kozhuharov, P.H. Mokler, Z. Stachura, and with the members of the ESR team, K. Beckert, B. Franzke, H. Reich, F. Nolden, and M. Steck. The author would like to thank J. Eichler for the close collaboration over many years and his continuous support with new and stimulating theoretical results.

REFERENCES

1. G. Raisbeck and F. Yiou, Phys. Rev. Lett. 4, 1858 (1971).
2. H. W. Schnopper, H. Betz, J. P. Devaille, K. Kalata, A. R. Sohval, K. W. Jones, and H. E. Wegner, Phys. Rev. Lett. 29, 898 (1972).
3. A. Ichihara, T. Shirai, and J. Eichler, Phys. Rev. A 54, 4954 (1996).
4. P. H. Mokler and Th. Stöhlker, Adv. in Atomic, Molecular, and Optical Physics, Vol.37, 297 (1996).
5. R. W. Schmieder, in *Proceedings of the NATO Workshop on the Physics of Highly Ionized Atoms, Cargese, Corsica June 1988*, edited by R. Marrus (Plenum Press: New York) 231 (1990).

6. Th. Stöhlker, F. Bosch, A. Gallus, C. Kozhuharov, G. Menzel, P.H. Mokler, H.T. Prinz, J. Eichler, A. Ichihara, T. Shirai, R.W. Dunford, T. Ludziejewski, P. Rymuza, Z. Stachura, P. Swiat, A. Warczak, Phys. Rev. Lett. 79, 3270 (1997).
7. R. H. Pratt, A. Ron, and H. K. Tseng, Rev. Mod. Phys. 45, 273 (1973).
8. B. Krässig, M. Jung, D. S. Gemmell, E. P. Kanter, T. LeBrun, S. H. Southworth, and L. Young, Phys. Rev. Lett. 75, 2736 (1995).
9. B. Craseman, X-Ray and Inner-Shell Process 1996 (AIP, Woodbury, New York, 1997), p. 3.
10. E. Spindler, H.-D. Betz and F. Bell, Phys. Rev. Lett. 42, 832 (1979).
11. J. Eichler and W. E. Meyerhof, *Relativistic Atomic Collisions* (Academic Press, San Diego, 1995).
12. J. Eichler, A. Ichihara, and T. Shirai, Phys. Rev. A 51, 3027 (1995).
13. A. Ichihara, T. Shirai, and J. Eichler, Phys. Rev. A 49, 1875 (1994).
14. S.J. Blakeway et al., J. Phys. B: At. Mol. Phys. 16, 3752 (1983).
15. H.K. Tseng, R.H. Pratt, S. Yu, A. Ron, Phys. Rev. A 17, 1061 (1978).
16. K. Blasche, B. Franzke, *Proc. of the 4^{th} Europ. Part. Acc. Conf.*, V. Suller and Ch. Petit-Jean-Genaz eds., World Scientific, Singapore, 1994, 133–137.
17. Th. Stöhlker, T. Ludziejewski, H. Reich, F. Bosch, R.W. Dunford, J. Eichler, B. Franzke, C. Kozhuharov, G. Menzel, P.H. Mokler, F. Nolden, P. Rymuza, Z. Stachura, M. Steck, P. Swiat, A. Warczak, Phys. Rev. A 58, 2043 (1998).
18. F. Bosch, Nucl. Instr. Meth. B 190, 23 (1987).
19. F. Bosch, Nucl. Instr. Meth. A 92, 314 (1992).
20. H. Reich, W. Bourgeois, B. Franzke, A. Kritzer, and V. Varentsov, Nucl. Phys. A 696, (1997).
21. Th. Stöhlker, C. Kozhuharov, P. H. Mokler, A. Warczak, F. Bosch, H. Geissel, R. Moshammer, C. Scheidenberger, J. Eichler, A. Ichihara, T. Shirai, Z. Stachura, P. Rymuza, Phys. Rev. A**51**, 2098 (1995).
22. Th. Stöhlker, T. Ludziejewski, F. Bosch, R. W. Dunford, C. Kozhuharov, P. H. Mokler, H. F. Beyer, O. Brinzanescu, B. Franzke, J. Eichler, A. Griegal, S. Hagmann, A. Ichihara, A. Krämer, J. Lekki, D. Liesen, F. Nolden, H. Reich, P. Rymuza, Z. Stachura, M. Steck, P. Swiat, A. Warczak, Phys. Rev. Lett. 82, 3232 (1999).
23. R. Anholt, S.A. Andriamonje, E. Morenzoni, Ch. Stoller, J.D. Molitoris, W.E. Meyerhof, H. Dowman, J.-S. Xu, Z.-Z. Xu, J.O. Rasmussen, D.H.H. Hoffmann, Phys. Rev. Lett. 53, 234 (1984).
24. Th. Stöhlker, H. Geissel, H. Irnich, T. Kandler, C. Kozhuharov, P.H. Mokler, G. Münzenberg, F. Nickel, C. Scheidenberger, T. Suzuki, M. Kucharski, A. Warczak, P. Rymuza, Z. Stachura, A. Kriessbach, D. Dauvergene, B. Dunford, J. Eichler, A. Ichihara, T. Shirai, Phys. Rev. Lett. **73**, 3520 (1994).
25. J. Eichler, Nucl. Phys. A 572, 147 (1994).
26. J. Eichler, A. Ichihara, T. Shirai, Phys. Rev. 58, 2128 (1998).
27. A. Krämer et al., to be published (1999).